Density of States-Based Model of Amorphous GaInZnO Thin Film Transistors by Using Optical Charge Pumping Technique

Jun-Hyun Park[1], Kichan Jeon[1], Sangwon Lee[1], Yong Woo Jeon[1], Changjung Kim[2], Ihun Song[2], Jaechul Park[2], Sunil Kim[2], Sangwook Kim[2], Youngsoo Park[2], Dong Myong Kim[1], and Dae Hwan Kim[1, a)]

[1]School of Electrical Engineering, Kookmin University, 861-1, Jeongneung-dong, Seongbuk-gu, Seoul, 136-702, KOREA [a)]drlife@kookmin.ac.kr

[2]Semiconductor Laboratory, Samsung Advanced Institute of Technology, Nongseo-Dong, Giheung-Gu, Yongin-Si, Gyeonggi-Do, 446-712, KOREA

Abstract

In order to model DC characteristics of *n*-channel amorphous GaInZnO (a-GIZO) thin-film transistors from experimentally obtained density of states (DOS), the acceptorlike DOS is extracted by using the optical charge pumping technique. Whereas the energy level is scanned by the photon energy and the gate voltage sweep, its density is extracted from the optical response of *C-V* characteristics. The extracted DOS shows the superposition of the exponential tail states and the Gaussian deep states. Furthermore, the TCAD simulation results incorporated by extracted DOS and a single set of process-controlled parameters show good agreements with the measured transfer and output characteristics of a-GIZO thin film transistors.

I. Introduction

Multi-component amorphous oxide semiconductor (*i.e.*, GaInZnO (GIZO), InZnO, and GaZnO)-based thin-film transistors (TFTs) have been under active research and development because of their room temperature (RT) fabrication process, higher mobility than those of covalent semiconductor TFTs, low cost, compatibility with transparent and rollable electronics applications. Because the electrical characteristics of GIZO TFTs are mainly dependent on both the electron concentration (n) and the density of states (DOS: $g(E)$) of the GIZO active layer, the extraction of n and $g(E)$ is very important in the modeling and characterization of their devices and circuits. Whereas the process parameter (*i.e.*, the oxygen partial pressure and/or the radio frequency (RF) power during RT sputtering process)-dependence of the carrier density (n_{Hall}) and the mobility (μ_{Hall}) by Hall measurement in GIZO thin-film have been well understood by many research groups [1-3], only a few groups have extracted $g(E)$ using numerical simulation-based fitting from experiment results [4-5]. In this work, an optical charge pumping technique based on capacitance-voltage (*C-V*) characteristic is proposed as a simple and fast method extracting accepterlike $g(E)$ in n-channel GIZO active layer.

II. Experimental Results and Discussion

A schematic cross-section of integrated GIZO TFTs is shown in Fig. 1 and has the most commonly used back-channel-etch staggered bottom gate structure for AMLCDs. On a thermally grown SiO_2/Si substrate, the first sputtered deposition at RT and patterning of molybdenum (Mo) gate are followed by PECVD deposition of a 100-nm-thick SiO_2 at 300°C (T_{GI}=100nm). A 70-nm-thick active layer (Ga_2O_3:In_2O_3:ZnO= 2:2:1 at %) is then sputtered by the RF magnetron sputtering at RT in a mixed atmosphere of Ar/O_2 (100:1 at sccm) and wet-etched with diluted HF (T_{GIZO}=70nm). For the source/drain (S/D) pattern, a 200-nm-thick layer of Mo is sputtered at RT and then patterned by dry-etching. After N_2O plasma treatment on the channel surface of the GIZO active layer, a SiO_2 passivation layer without a vacuum break is continuously deposited at 150 °C by PECVD, and finally, all the samples were annealed at 250 °C for 1 hr in the furnace. The channel length (L), the channel width (W), and the length of the overlap region between the gate and S/D (L_{ov}) are designed to be 50, 90~200, and 10 μm, respectively. Fabricated GIZO layer has an amorphous phase (a-GIZO) with XRD and TEM views, and shows the nature of *n*-type amorphous oxide semiconductor.

Illustrative concept of the extraction of a-GIZO $g(E)$ based on an optical charge pumping technique as shown in Fig. 2. An optical source with a sub-bandgap photon energy (λ=654 nm, E_{ph}=1.90 eV<$E_{g,GIZO}$≈3.2 eV) is employed to pump trapped electrons in localized states $g(E)$ from the energy level below the Fermi level E_F to the a-GIZO conduction band minimum (CBM) E_C by the specific E_{ph} while excluding the band-to-band electron-hole pair generation in the a-GIZO layer. By modeling C_{dark} and C_{photo} as (1)~(2), C_{GIZO} can be extracted as a function of V_{GS} from (3) in Table I (detailed definitions of parameters are given in Table I). Since C_{ox} can be calculated, C_{GIZO} can be also extracted from Eq. (3). As a result of the conversion of ΔN to the photo-responsive electron density Δn [cm^{-3}] with (4)~(5), $g(E)$ is extracted by using (6), where r (=25 μm), $E_F(V_{GS})$, and ΔV_{GS} (=303 mV) are the radius of the optical fiber used in the photon-illumination, the quasi-Fermi level as a function of V_{GS}, and the resolution of swept V_{GS} in the *C-V* measurement, respectively. As seen in Eqs. (4)~(6), we note that the photo-responsive energy range of $g(E)$ is modulated by both the surface potential (ϕ_s) through V_{GS} and E_{ph}. The $g(E)$ is assumed to be uniformly distributed along the a-GIZO depth direction and this is valid as far as the energy band bending is not so steep over the region. In terms of matching the energy level, two transition points in the *C-V* curve are assumed to correspond to E_i (midgap) and E_C, respectively, as shown in the inset of Fig. 2.

In order to confirm a comprehensible charge pumping by the optical source, the optical power (P_{opt}) and frequency (f)-dependence of C_{photo}-V_{GS} curves should be taken into account. Fig. 3(a) shows that the C_{photo}- V_{GS} characteristic becomes insensitive to the frequency at f > 700 Hz. Fig. 3(b) shows that the optical response of the C_{photo}- V_{GS} curves saturates at P_{opt}>41 mW, and this guarantees that the trapped charges in corresponding energy levels are sufficiently excited by photons. Fig. 4 shows the optical response of *C-V* characteristics of a-GIZO TFTs with different W (90 and 200 μm) at f=700 kHz and P_{opt}=50 mW. Fig. 5(a) shows the $g(E)$ extracted from Fig. 4, which is a superposition of the exponential tail states and the Gaussian deep states, as is the case in a-Si:H TFT's [6]. In the *C-V* curve under P_{opt}=50 mW for V_{GS}=-5 V and 1.4 V (the value of 1.4 V was consistent with the linearly extrapolated threshold voltage V_T) are matched to E_i and E_C, respectively, assuming that ϕ_s is a function proportional to V_{GS}. In addition, Fig. 5(b) shows an effective mobility $\mu_{EFF}(V_{GS})$ used in our model compared with the measured field-effect mobility $\mu_{FE}(V_{GS})$. The V_{GS}-dependent mobility in a-GIZO TFTs is originated from the incremental portion of filled localized states among total states. Consequently, extracted $g(E)$ is modeled as Table II. It is also noticeable that the $g(E)$ extracted from proposed technique is independent of W/L as shown in Fig. 5(a).

In Fig. 6, measured output and transfer characteristics of a-GIZO TFTs are compared with the model obtained from TCAD simulation (Silvaco ATHENA and ATLAS) [7] incorporating the extracted $g(E)$. The model reproduces measured characteristics very well for a wide range of V_{GS} and V_{DS} by considering the consistent process-controlled parameters including the effective density of states in the conduction and valence bands N_C=N_V=10^{19} cm^{-3}, n=3.98×10^{16} cm^{-3}, and ϕ_B (Schottky barrier height)=2.7 eV (Note that a single parameter set, not fitting parameters, is used with various V_{GS}/V_{DS}).

III. Conclusions

The acceptorlike $g(E)$ of *n*-channel a-GIZO TFT was successfully extracted by using the optical charge pumping

technique. In addition, the validity of the extracted $g(E)$ was verified by its incorporation into TCAD simulation and comparison with the measured transfer and output characteristics. Our results show that the proposed DOS-based model is very useful for the device design and modeling of a-GIZO TFTs.

Acknowledgements

This work was supported by the research project of Samsung Advanced Institute of Technology, and the CAD softwares by SILVACO and IC Design Education Center (IDEC).

References

[1] Y. Orikasa *et al*., J. Appl. Phys., vol. 103, no. 11, pp. 113703-1-7, 2008.
[2] K. Nomura *et al*., Nature, vol. 432, no. 7016, pp. 488-492, 2004.
[3] E. Fortunato *et al*., Thin Solid Films, vol. 502, no. 1/2, pp. 104-107, 2006.
[4] H.-H. Hsieh *et al*., *Appl. Phys. Lett.*, vol. 92, no. 13, pp. 133503-1-3, 2008.
[5] M. Kimura *et al*., *Appl. Phys. Lett.*, vol. 92, no. 13, pp. 133512-1-3, 2008.
[6] C. R. Kagan and P. Andry, *Thin-Film Transistors*. New York: CRC, 2003, pp. 77-78.
[7] *Atlas Users Manual*, Silvaco International, Santa Clara, CA, 2005. [Online]. Available: http://www.silvaco.com

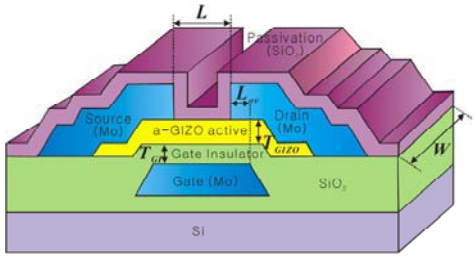

Fig. 1. Schematic diagram of the integrated a-GIZO TFTs.

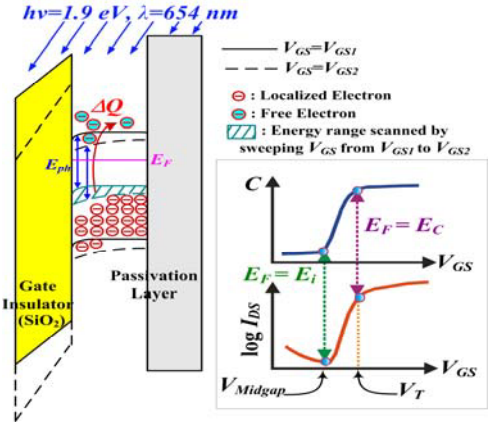

Fig. 2. Illustrative concept of the extraction of a-GIZO $g(E)$ based on an optical charge pumping technique. The trapped electrons in specific energy levels (Δn) that would not response in a dark condition (C_{dark}) are excited to the levels above E_F and response under the optical pumping (C_{photo}). The range of energy level can be controlled by both E_{ph} and V_{GS}.

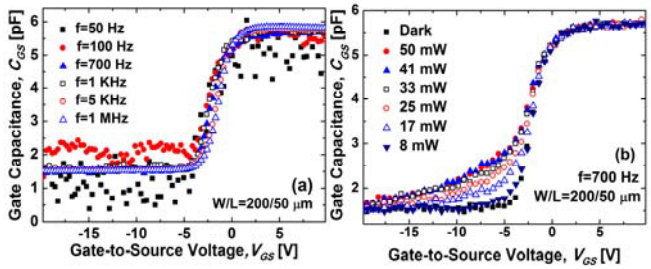

Fig. 3. (a) The frequency and (b) the optical power P_{opt} dependence of C-V measurement in a-GIZO TFTs.

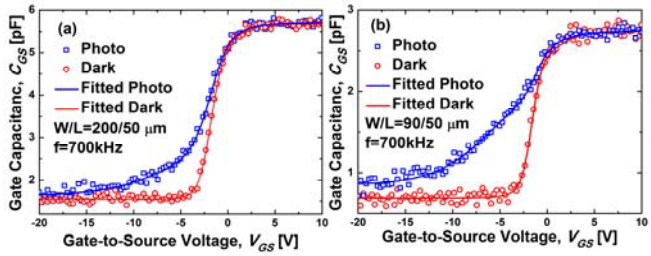

Fig. 4. The measured optical response of C-V curve at P_{opt}=50 mW.

Table I. Used model equations

Equations
$\frac{1}{C_{dark}(V_{GS})}=\frac{1}{C_{ox}}+\frac{1}{C_B(V_{GS})}$ (1)
$\frac{1}{C_{photo}(V_{GS})}=\frac{1}{C_{ox}}+\frac{1}{C_B(V_{GS})+C_{GIZO}(V_{GS})}$ (2)
$C_{GIZO}(V_{GS})=\frac{\Delta Q}{\Delta V_{gs}}=\frac{q\Delta N}{\Delta V_{gs}}=C_{ox}\left[\frac{C_{photo}}{C_{ox}-C_{photo}}-\frac{C_{dark}}{C_{ox}-C_{dark}}\right]$ (3)
$\Delta N(V_{GS})=\pi r^2\times T_{GIZO}\int_{E_C(V_{GS})-E_{ph}}^{E_F} g(E)dE$ (4)
$\Delta C_{GIZO}{}'=\frac{C_{GIZO}(V_{GS2})-C_{GIZO}(V_{GS1})}{\pi r^2\times T_{GIZO}}=\frac{q\Delta n}{\Delta V_{GS}}=\frac{q\int_{(E_F-E_i)(V_{GS1})}^{(E_F-E_i)(V_{GS2})} g(E)dE}{\Delta V_{GS}}$ (5)
$g(E)=\frac{\Delta C_{GIZO}{}'}{q^2},\quad (E_F-E_i)(V_{GS1})<E<(E_F-E_i)(V_{GS2})$ (6)
C_{ox} : Gate oxide insulator capacitance [F] C_B : Capacitance due to V_{GS}-responsive localized trapped charge in the a-GIZO active layer [F] C_{GIZO} : Capacitance due to photo-responsive charge (ΔQ) at a fixed V_{GS} (see Eq. (3)) [F] C_{dark} : Measured capacitance in a dark state C_{photo} : Measured capacitance in a photon-illuminated state ΔQ and ΔN : Photo-responsive charge and electrons C_{GIZO}' : Capacitance per unit volume due to photo-responsive charge (ΔQ) at a fixed V_{GS} ([Fcm^{-3}] $g(E)$: Density of states of the a-GIZO active layer [cm$^{-3}\cdot$eV^{-1}]

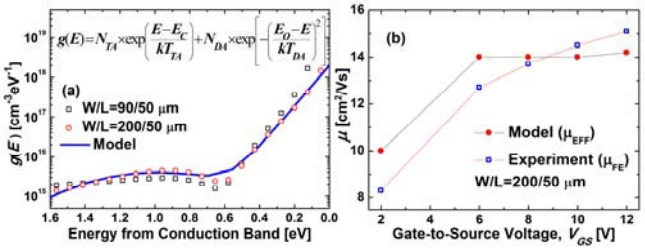

Fig. 5. (a) The extracted $g(E)$ for a-GIZO TFTs with different W/L (inset: $g(E)$ equation). (b) Comparison of measured field effect mobility (μ_{FE}) with the effective mobility (μ_{EFF}) used in the DOS-based model.

Table II. $g(E)$ model for a-GIZO TFTs with W/L=200/50 μm

Model and Parameter Values
$g(E)=N_{TA}\times\exp\left(\frac{E-E_C}{kT_{TA}}\right)+N_{DA}\times\exp\left[-\left(\frac{E_O-E}{kT_{DA}}\right)^2\right]$
N_{TA}=2×10^{18} [cm$^{-3}\cdot$eV^{-1}], N_{DA}=4×10^{15} [cm$^{-3}\cdot$eV^{-1}] kT_{TA}=0.085 [eV], kT_{DA}=0.5 [eV], E_O=1 [eV]

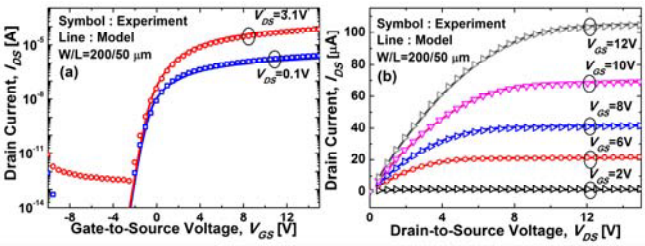

Fig. 6. (a) Measured transfer characteristics and (b) output characteristics of a-GIZO TFT's. The model agrees well with measured characteristics.